

A green approach to Synthesize Cellulose Nano Crystals –Loaded Poly (Vinyl Alcohol) Films with Enhanced Stability

Abstract

In this work, poly (vinyl alcohol)(PVA) films have been rendered with insoluble character by introducing cellulose nano-crystals(CNC), obtained by ultra-sonication of cellulose powder in aqueous medium at room temperature. The films, thus produced, were quite stable against dissolution in aqueous medium for more than 7 days, while the plain PVA films were fully dissolved in a short period of 30 min. The films were characterized by FTIR, XRD and SEM analysis. The water absorption behavior of films was studied in the physiological fluid (PF) of pH 7.4. The films, loaded with 12, 24 and 30 wt % of CNC exhibited swelling ratio (SR) of 0.80, 1.33 and 0.96 g/g respectively, thus showing unusual trend. The kinetic water uptake data were analyzed by Power function model which revealed that the water transport mechanism was less-diffusion controlled. In addition the Schott model was found to fit well and the parameters evaluated were quite close to the experimental data.

Keywords: Hydrogel Films, Cross-Linking, Water Uptake Analysis, Less-Fickian Swelling, Physiological Fluid (PF).

Introduction

Poly (vinyl alcohol) is a biocompatible and biodegradable polymer, usually obtained by hydrolysis of poly(vinyl acetate)¹. The degree of substitution (DS) governs its physico-chemical properties to a large extent. Indeed, PVA has been widely employed in a large number of biomedical applications due to its biodegradable and biocompatible nature. These applications include drug delivery *vitro*²⁻⁵, tissue engineering⁶, wound dressings⁷, porous scaffolds⁸ etc. In addition, PVA is also used for food packaging⁹. In spite of having excellent film forming property, mechanical strength and water absorption behavior, PVA films suffer from a major drawback that they have a very strong dissolution tendency in aqueous medium. This restricts its use for applications such as drug delivery and wound dressings where the polymers has to maintain its structural integrity in physiological fluid for a long time period while delivering the entrapped biologically active ingredients. This problem is usually overcome by carrying out chemical cross-linking of PVA with an appropriate cross-linker such as formaldehyde, glutaraldehyde, epichlorohydrin etc.¹⁰ This is a most adopted strategy to prevent the PVA hydrogel from dissolution and has been used frequently in various biomedical applications. For example, Garnica-Palafox et al.¹¹ have investigated mechanical properties of PVA/chitosan hydrogels cross-linked with epichlorohydrin. In another work, Kumar and co-worker¹² have produced PVA, sodium alginate and chitosan based hydrogels cross-linked by glyoxal. The films were characterized by various analytical techniques. In order to avoid using toxic cross-linking agents, attempts have been made to modify PVA using non-toxic chemicals. For example, most recently, Zhang et al.¹³ have modified PVA by grafting it with succinate acid to yield carboxyl-modified poly (vinyl alcohol) (PVA-COOH). This was later used as a cross-linker to prepare chitosan based hydrogels via amide linkage formation. In another strategy, H-bonding interactions have been employed as physical cross-links to prevent PVA based hydrogels from dissolution. Most recently, Tian et al.¹⁴ have prepared PVA/starch blends by melt process and reported their physico chemical properties. The H-bonding interactions between starch and PVA affected properties of blends.

J. M. Kellar

Designation- Fill....

Deptt.of Physics,
University Teaching Department,
Rani Durgawati Vishwavidyalaya,
Jabalpur , M.P.

Nema Mishra

Research Scholar,
Deptt.of Physics,
University Teaching Department,
Rani Durgawati Vishwavidyalaya,
Jabalpur , M.P.

In the present work, we have used cellulose nano crystals as an additive to not only strengthen the PVA films but also to prevent them from dissolution. Cellulose is the most abundantly found bio-polymer in nature and is biocompatible and biodegradable¹⁵. It has frequently been used in a number of biomedical applications. It is speculated that presence of a large number of hydroxyls along its backbone may bind to the -OH groups of PVA chains through H-bonding interactions to serve as additional cross-links and provide stability to PVA hydrogels.

Objectives of the Study

Poly (vinyl alcohol) is a biocompatible, polymer with excellent film forming properties. However, it has to be crosslinked with toxic cross-linkers like glutaraldehyde, formaldehyde etc. in order to prevent the films against dissolution. In this work, for first time we have produced insoluble films by loading cellulose nanocrystals into PVA films without using any toxic chemical. The CNC were prepared by physical method, i.e. ultra sonication of cellulose suspension in water. Their mechanical and water absorption properties were also studied.

Review of Literature

A review on polymeric hydrogel membranes for wound dressing applications: PVA-based hydrogel dressings. Kamoun EA, Kenawy ES, Chen X. J Adv Res. 2017 May;8(3):217-233]

Characterisation and in stability of low-dose, lidocaine-loaded poly (vinyl alcohol)-tetrahydroxyborate hydrogels. Abdelkader DH, Osman MA, El-Gizawy SA, Faheem AM, McCarron PA. Int J Pharm. 2016 Mar 16;500(1-2):326-35, Poly(vinyl alcohol) Physical Hydrogels: Matrix-Mediated Drug Delivery Using Spontaneously Eroding Substrate. Jensen BE, Dávila I, Zelikin AN. J PhysChem B. 2016 Jul 7;120 (26):5916-26, Synthesis and characterisation of cationic quaternary ammonium-modified polyvinyl alcohol hydrogel beads as a drug delivery embolisation system. Heaysman CL, Phillips GJ, Lloyd AW, Lewis AL. J Mater Sci Mater Med. 2016 Mar;27(3):53.],

Experimental

Materials

Poly (vinyl alcohol) (PVA; degree of substitution 95 %), cellulose powder; Cell), and other chemicals were purchased from Hi Media Chemicals, Mumbai, India. The double distilled water was used throughout the investigations.

Preparation of Cellulose Nano Crystals

The cellulose nanocrystals were prepared by ultra-sonication method¹⁶. In brief, 2 g of cellulose powder was dispersed in 50 mL of distilled water and ultrasonicated at a frequency of 4 h per day till the cellulose particles remained suspended and did not show any tendency to settle down. The suspension was stored in a dust free chamber till further use.

Preparation of CNC/PVA composite films

The CNC/PVA composite films were prepared by solvent evaporation method. In brief, 10 % (wt/vol) PVA solution of PVA was prepared in distilled water. Now, definite volumes of the above prepared CNC suspension and PVA solution were mixed under moderate stirring to give a total volume

of 50 mL. The solutions were poured into Petri plates and put in electric oven (Temp star, India) at 60°C for a period of 4 h. The films, so prepared, were peeled off carefully and placed in a dust free chamber for further use. In all four samples were prepared, designated as CNC/PVA(x), where x is the wt % of CNC in the film with respect to PVA content. The films shall be designated as CNC/PVA (0), CNC/PVA(12), CNC/PVA(18) and CNC/PVA(24).

Characterization of CNC/PVA(x) Films

The Fourier Transform Infrared (FTIR) spectra were recorded with an FTIR spectrophotometer (Shimadzu, 8400, Japan) using KBr. The powdered sample was mixed with KBr. The scans recorded were the average of 100 scans and the selected spectral range between 400 to 4000 cm⁻¹.

The X-ray diffraction (XRD) method was used to measure the crystalline nature of the films. These measurements were carried out on a Rikagu Diffractometer (Cu radiation = 0.1546 nm) running at 40 kV and 40 mA. The diffractogram was recorded in the range of 2θ from 3 to 50° at the speed rate of 2 degree/ min.

In order to investigate the surface morphology of films, SEM and AFM images were recorded at IISER, Pune (Maharashtra State), India.

Swelling studies

Swelling studies were carried out in the pseudo extracellular fluid (PEF) as described by Lin et al.¹⁷. This simulated wound fluid has following composition : 2.2 g of KCl, 6.8 g of NaCl, 25 g of sodium bicarbonate and 3.5 g of sodium di-hydrogen phosphate in 1 liter. The pH of this solution was found 7.36. The pre-weighed film sample was placed in 100 mL of PEF at 37°C and it was taken out at different time intervals, wiped superficially with tissue paper to remove extra surface water, weighed accurately in an electronic balance (Denber, Germany), and then placed back in water. The swelling Ratio (SR) determined at different time intervals using the following expression:

$$SR = \frac{(m_t - m_0)}{m_0} \text{g/g} \quad \dots (1)$$

Where m_0 and m_t are the initial mass and mass at different time intervals respectively. In order to determine Equilibrium Swelling Ratio (ESR), m_t was replaced by m_e which is the weight of the swollen film at equilibrium.

Results and discussion

Preparation of cellulose nano crystals

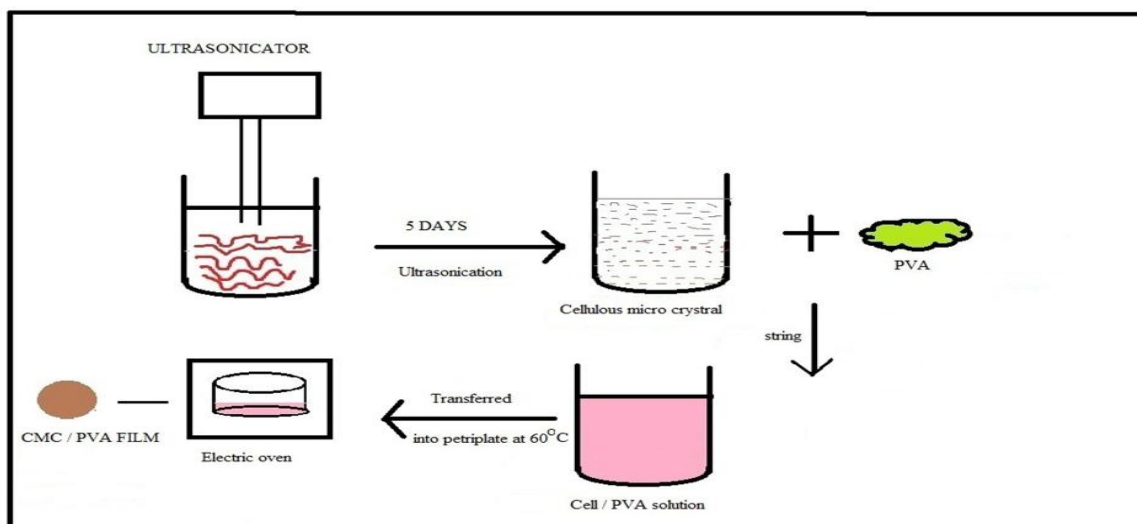
According to the literature available, cellulose nano crystals have been prepared by a number of methods such as acidhydrolysis¹⁸, mechanical disintegration¹⁹, enzymatic hydrolysis [20] etc. However, the mechanical disintegration appears to be the safest one as it is pro-ecofriendly approach. In this work, cellulose particles were ultrasonicated for total period of 5 days, with an exposure frequency of 5 h per day which enabled us to obtain cellulose nano crystals. The ultrasonic waves penetrate through the amorphous region of cellulose chains and break them in to smaller sized chains with dimension in the nano scale range.

Preparation of CNC/PVA films

In the present work, Cellulose nano crystals have been well dispersed in to PVA film matrix. The film forming solution consists of well dispersed CNCs in the aqueous solution of PVA. When the solution is poured in to Petri plates and the solvent is evaporated, the CNC/PVA film is produced. Here, it

may be considered that -OH groups along the PVA chains may act as templates to bind with cellulose nano crystals through H-binding interactions. After the solvent is evaporated, a uniformly distributed array of cellulose nano crystals is obtained within the film. The proposed scheme for formation of CNC/PVA film is shown in Fig.1.

Figure 1

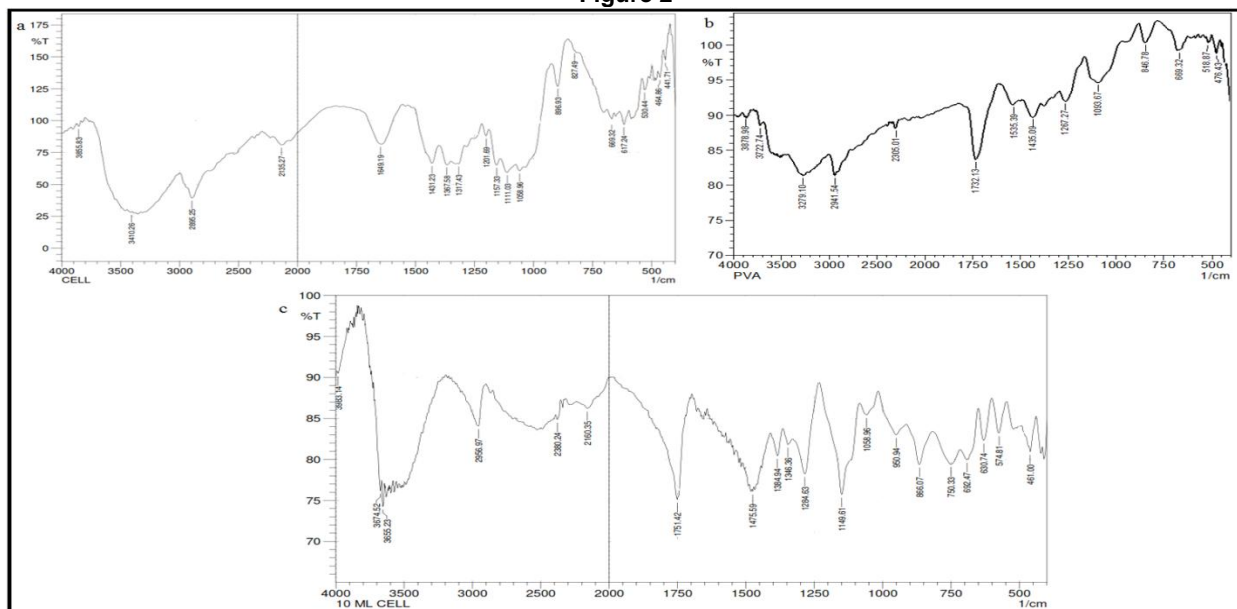


Characterization of films

The FTIR spectra of pure cellulose, native PVA and CNC/PVA (18) film are shown in Fig. 2(a) (b) and (c) respectively. It can be observed in Fig. 2(a) that there is a strong broad band at around 3410 cm⁻¹, which is assigned to different O-H stretching modes. The characteristic peak at 2896 cm⁻¹ shows C-H, CH₂ stretching of cellulose. The bands at 1431,

1317, 1201 and 1111 cm⁻¹ are characteristic of C-H, C-O deformation, bending or stretching vibrations of many groups in lignin and carbohydrates²¹. The bands at 1367, 1201, 1157 and 1058 cm⁻¹ are assigned to C=O, C-H, C-O-C and C-O deformation or stretching vibrations of different groups in carbohydrates²².

Figure 2



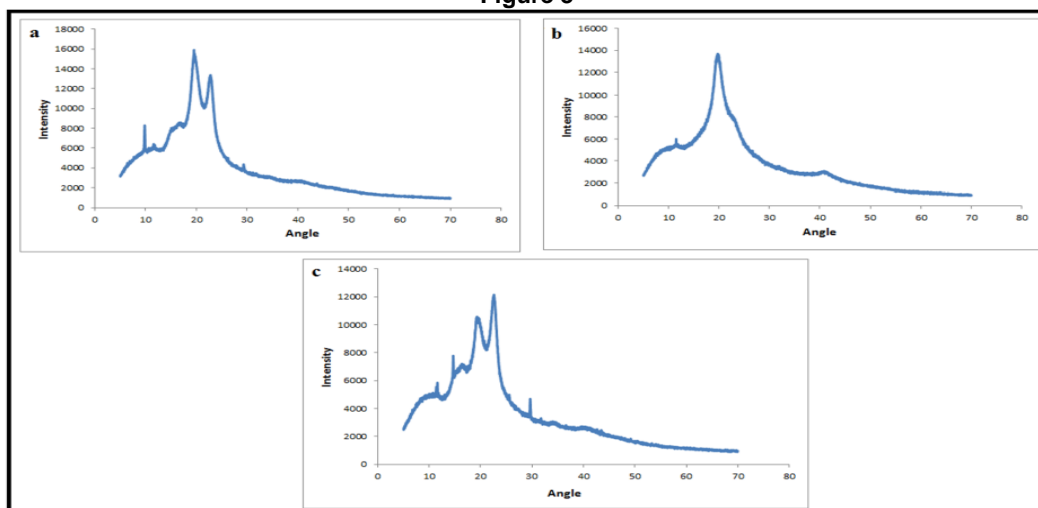
Finally, absorption band at 897 cm⁻¹ is assigned to -C-O-C stretching at β-(1→4) glycosidic linkage[23]. In the spectrum of PVA, as shown in Fig.2 (b), the 3279 cm⁻¹ and 2941 cm⁻¹ are the -OH and CH₂ stretching vibrations. The C-O stretching range is at

1093 cm⁻¹. The spectrum of composite film, displayed in Fig.2 (c) reveals that C-H alkyl stretching band appears at 2956 cm⁻¹ (ν = 2850-3000 cm⁻¹), superimposing the sharp peak obtained due to C-H, CH₂ stretching of native cellulose. It is also noticed

that typical strong hydroxyl bands for free alcohol (non-bonded -OH stretching band at $\nu = 3600-3650 \text{ cm}^{-1}$), and hydrogen bonded band ($\nu = 3200-3570 \text{ cm}^{-1}$) also appear in the spectrum of composite film. In addition, the C-O stretching, a characteristic peak for PVA, appears at approximately 1111 cm^{-1} . The diffraction pattern of native cellulose, shown in Fig.3(a), confirm relatively suppressed peak at $2\theta = 14.62^\circ(1\bar{1}0)$ and a sharp peak at $22.48^\circ(200)$, thus indicating the presence of cellulose I.[24]. In addition a sharp peak also appears at $2\theta = 21.53 (200)$,

indicating presence of cellulose II structure[25]. The XRD pattern of the pure PVA film, as shown in Fig.3(b) indicates strong crystalline reflections at around $2\theta = 19.92^\circ$ and a shoulder at 22.74° . The two peaks are characteristic of PVA, representing reflections from (101) and (200) from monoclinic unit cell [26]. Finally, the XRD pattern of CNC/PVA(18), displayed in Fig.3(c) indicates presence of nearly all the peaks that exist in diffractogram of cellulose and PVA as mentioned above.

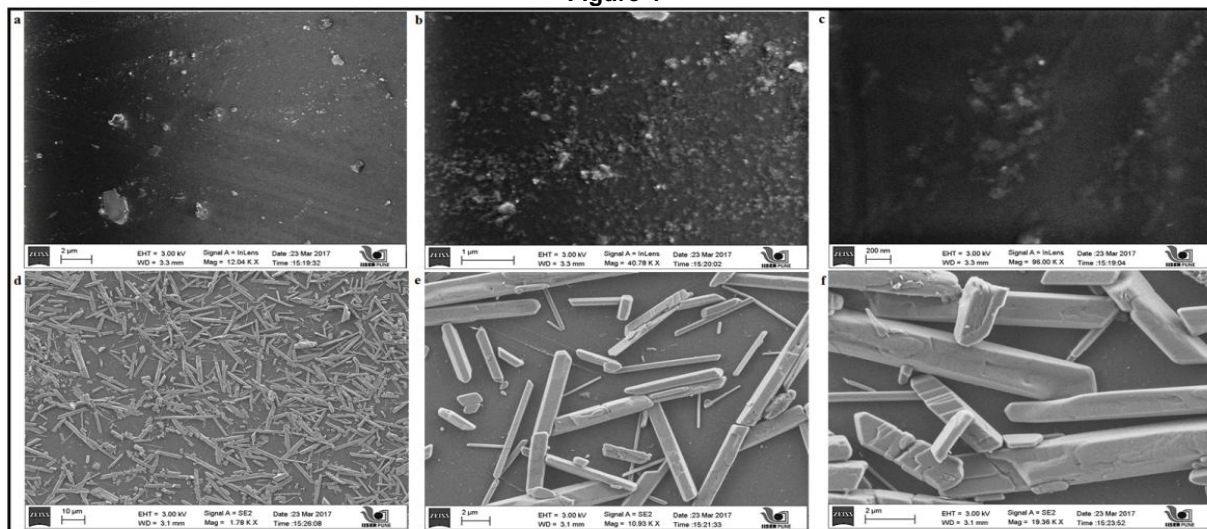
Figure 3



The Scanning electron microscopy (SEM) was carried out to investigate surface texture of the plain and CNC loaded films. The results for the plain CMC/PVA(0) are shown in Fig.4(a-c) with magnifications of 12000, 40000 and 96000

respectively. The surface texture, shown in Fig.2(a) indicates a little rough surface with a little agglomeration at some places, probably due to the presence of some impurities or un-dissolved PVA crystals.

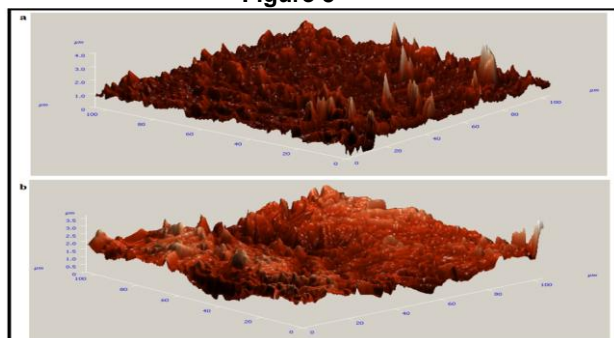
Figure 4



The Fig. 4(b) also supports this observation. Finally, the image, displayed in Fig.4(c) reveals that the particulates are up to 500 nm. The SEM images of sample CNC/PVA(18) are displayed in Fig.4(d-f) with relative magnifications of 1780, 10930 and 19360 X respectively. It can be observed in Fig.4(d) that the cellulose crystals are almost uniformly distributed throughout the film matrix, though at some places the density is not so high as compared to other

places. A further observation at still higher magnifications, displayed in Fig.4(e-f) reveal that cellulose crystals have bar-like geometry and some crystals quite differ in size and dimensions. In order to further confirm the surface texture of the PVA and CNC/PVA films, we also recorded their AFM images. The results are shown in fig.5 for the plain and the CNC/PVA films respectively.

Figure 5



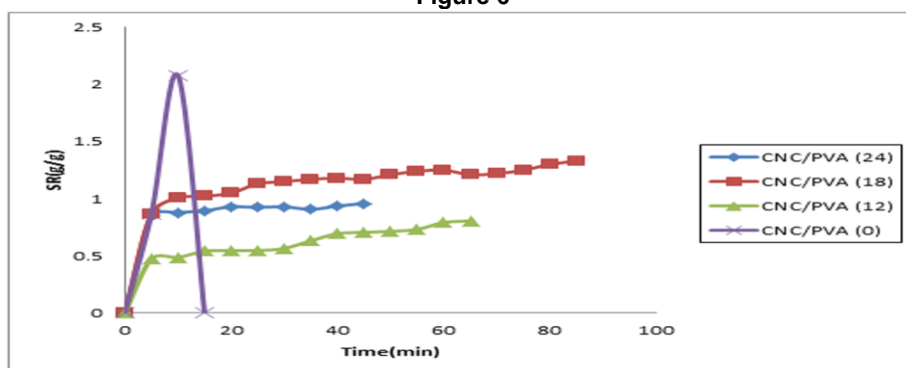
In the AFM image of PVA film grooves up to the height of 350 nm could be observed throughout the film matrix. On the other hand, AFM image of CNC/PVA film indicates uniform grooves up to the height 4 μm thus suggesting an almost rough surface due to the presence of cellulose micro-crystals. In this

way, it may be concluded that plain PVA film has relatively smooth surface while the CNC-loaded PVA film has rough surface throughout due to the presence of micrometer sized cellulose crystals.

Swelling kinetics of CNC/PVA Composite Films

The water absorption behavior of plain PVA and CNC/PVA films containing different cellulose contents were studied in the phosphate buffer saline(PBS) of medium 7.4. The results are shown in Fig.5. It can be seen that the plain PVA film shows a faster swelling and attains ESR of 2.1 in 15 min. However, thereafter it begins to lose weight and dissolves completely in next 5 min. On the other hand, the film samples CAN/PVA(12), CNC/PVA(18) and CNC/PVA(24) show total swelling ratios of 0.80, 1.33 and 0.95 g/g respectively. It took almost 45 to 80 min for the samples to attain equilibrium swelling ratio (ESR).

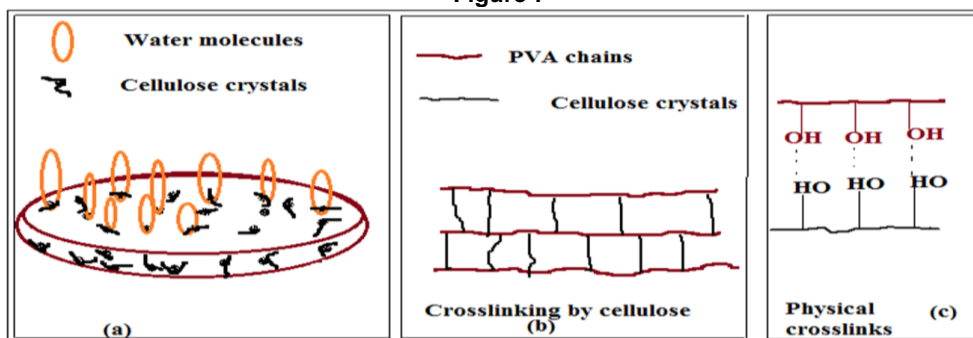
Figure 6



The observed swelling data for the film samples CAN/PVA(12), CNC/PVA(18) and CNC/PVA(24) suggest that as the cellulose content in the film increases from 12 to 18 % (w/v), the ESR also increases. However, with the further increase in the cellulose content to 24 %(w/v), the ESR begins to decrease. The results may be explained as follows. Initially, the increase in CNC content from 12 to 18 % causes an increase in the surface hydroxyls due to presence of cellulose. These –OH groups interact with incoming water molecules and bind to them, thus resulting in higher water uptake. In addition, the added cellulose crystals also impart stability to the film by establishing physical cross-links with the –OH groups of PVA chains. However, as the cellulose content is further increased from 18 to 24 wt %, the cellulose crystals produce, present within the bulk of

the film matrix, and produce more physical cross-links through H-bonding interactions with hydroxyls of PVA chains. These physical cross-links result in a decrease in the free space available for accommodation of incoming water molecules. In addition relaxation of PVA chains is also restricted due to increased cross-linking. It is also noteworthy that all the three samples, containing cellulose within the film matrix, show enhanced stability for more than 72 h, while the pure PVA film just dissolves in 15 min. Therefore it may be concluded that addition of cellulose nanocrystals in to the PVA film matrix, causes the films to be highly stable in aqueous medium. The schematic illustration of interactions of cellulose molecules with PVA chains within the film samples CAN/PVA(120), CNC/PVA(18) and CNC/PVA(24) is shown in Fig.7.

Figure 7



It may be observed in Fig.7 (a) that water molecules, entering in to the film matrix are attached to the surface hydroxyls of cellulosic micrometer sized crystals, thus enhancing the water absorption behavior. However, as the cellulose content increases, the cellulose microcrystals produce additional cross-links (see Fig.7(b)). These physical cross-links are well illustrated in Fig.7(c).

Modeling of the Water Uptake Data

The water penetration mechanism of the CNC/PVA films was best investigated using the well-

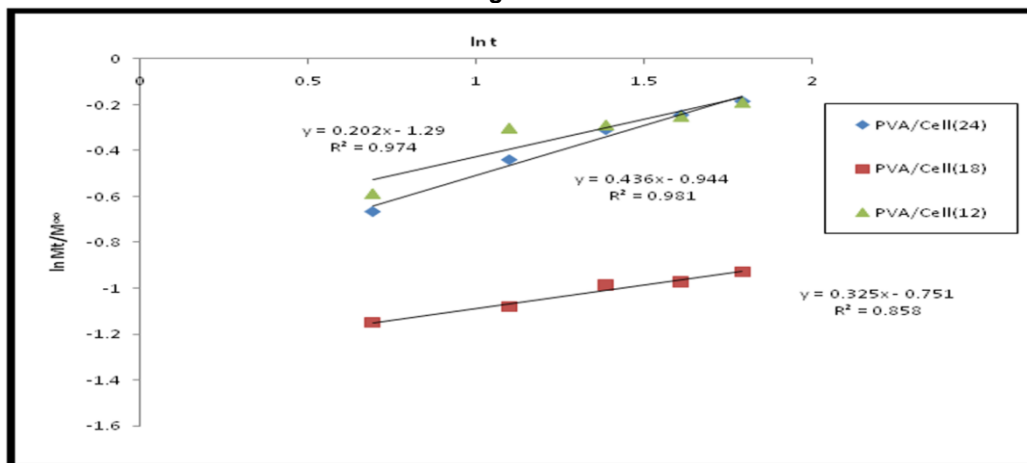
known "Power function model", developed by Peppas[27].According to this model

$$\frac{M_t}{M_\infty} = k t^n \dots (2)$$

Where M_t and M_∞ are the masses of the hydrated film sample at time 't' and at equilibrium respectively; 'n' and 'k' are the swelling exponent and gel-characteristic constants respectively. The logarithmic form of the above equation may be written as

$$\ln \frac{M_t}{M_\infty} = \ln k + n \ln t \dots (3)$$

Figure 8



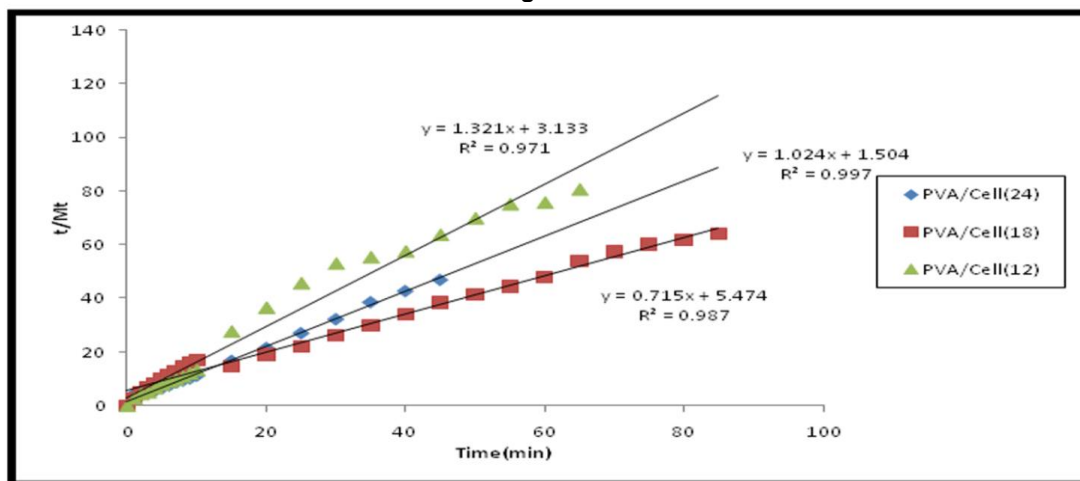
The initial 60% water uptake data was used to draw linear plots between $\ln M_t / M_\infty$ and $\ln t$, which yielded straight lines with fairly higher regressions., as shown in Fig.7. It was observed that the swelling exponent 'n' for the samples CAN/PVA (120), CNC/PVA(18) and CNC/PVA(24) was found to be 0.20, 0.32 and 0.41 respectively. These values are quite below than 0.5, thus suggesting 'less Fickian' behavior of the films. This indicates that for all the three film samples, rate of diffusion of water into hydrogel films is much smaller than the rate of relaxation of polymeric chains. This may be explained on the basis of the facts that poly (vinyl alcohol) chains undergo faster relaxation due to strong interactions with incoming water molecules. But the diffusion of water into the matrix takes place at very

slow rate due to presence of cellulose crystals which act as diffusion barrier for the incoming water molecules. Similar results have also been reported for medium molecular weight chitosan films that were cross-linked by tri-poly phosphate ions. Their swelling exponent in the buffer medium of pH 7.4 was found to be 0.35, thus indicating 'less Fickian water penetration mechanism'[28].Almost similar results were also reported in our previous work for the swelling behavior of PVA/Carrageenan cross-linked hydrogel films[29].All the related parameters for the three film samples are given in Table-I.

The Schott kinetic model was also applied on the kinetic water absorption data. According to this model [30]:

$$dM_t/dt = k_2 (M_\infty - M_t)^2 \dots (4)$$

Figure 9



Where, M_t is the water uptake at time 't' and ' k_2 ' is the second order rate constant for water absorption process. On integrating above equation within the limits $t=0$ $M_t=0$ and $t=\infty$ $M_t=M_\infty$, following equation is obtained:

$$t/M_t = 1/k_2 M_\infty^2 + t/M_\infty$$

Or

$$t/M_t = A + B t \quad \dots (5)$$

Where, A and B are two coefficients whose physical meaning is interpreted as follows: At a long retention time $Bt \gg A$ and therefore $B = 1/M_\infty$, that is, B is reciprocal of the maximum water uptake. On the contrast, at a very short time interval $Bt \ll A$ and so,

$$Lt (dM_t/dt) = 1/A \quad \dots (6)$$

$t \rightarrow 0$

Therefore, the intercept A is reciprocal of initial swelling rate. In order to apply this model, the kinetic data were used to draw plots between t/M_t and t as shown in Fig.6. The slopes and intercepts of linear plots were employed to evaluate the rate constant k, equilibrium water uptake M_∞ and initial swelling rate (i.e. $r_{ini} = 1/A$). All these parameters are shown in Table-I. A close look at the various parameters, obtained for the Schott model, reveals that for all the samples regressions are fairly high thus indicating the suitability of the Schott model. In addition, it may also be noticed that the theoretical and experimental SR values are quite close to each other, thus further confirming the validity of this model.

Conclusion

It may be concluded from the above study that entrapment of cellulose microcrystals in to un-cross-linked poly(vinyl alcohol) film renders it with fair stability in the physiological fluid while the un-cross-linked film dissolves within 20 min after its immersion. In addition, the water absorption behavior of CMC-reinforced PVA films follows Fickian water transport mechanism. Since the PVA films have been stabilized through entrapment of cellulose micro-crystals, and no toxic chemical has been used throughout the study, these films have great potential to be used for biomedical applications.

References

1. Kamoun, E. A., Kenawy, E. S., Chen, X., (2017) PVA-based hydrogel dressings, *J Adv Res.* 8(3):217-233.
2. Martínez-Gómez, F., Guerrero, J., Matsuhira, B., Pavez, J., (2017) *Carbohydr Polym.* 155:182-191
3. Abdelkader, D. H., Osman, M.A., El-Gizawy, S. A., Faheem, A. M., McCarron, P.A., (2016) *Int J Pharm.* 500(1-2):326-35.
4. Jensen, B.E., Davila, I., Zelikin, A.N., *Phys Chem, B.J.*, (2016) 120(26):5916-26.
5. Heaysman, C.L., Phillips, G.J., Lloyd, A.W., Lewis, A.L., (2016) *J Mater Sci Mater Med.* 27(3):53.
6. Kumar, A., Han, S. S., (2017) *International Journal Of Polymeric Materials And Polymeric Biomaterials.* 66: 159-182.
7. Kamoun, E.A., Kenawy, E.S., Chen, X., (2017) *J Adv Res.* 8(3): 217-233.
8. Lin, H.Y., Tsai, W.C., Chang, S.H., etc. (2017) *J Biomater Sci Polym Ed.* 28(7):664-678.
9. Wu, Z., Wu, J., Peng, T., Li, Y., Lin, D., Xing, B., Li, C., Yang, Y., Yang, L., Zhang, L., Ma, R., Wu, W., Lv, X., Dai, J., Han, G., (2017) 102-121.
10. Kamoun, E.A., Chen, X., MohyEldina, M. S., Kenawy, E. S., (2015) *Arabian Journal of Chemistry* 8(1): 1-14.
11. Garnica-Palafox, I. M., Sánchez-Arevalo, F.M., Velascoquillo, C., García-Carvajal, Z. Y., García-Lopez, J., Ortega-Sánchez, C., Ibarra, C., Luna-Barcenas, G., Solís-Arrieta, L., (2014) *J Biomater Sci Polym Ed.* 25(1):32-50,
12. Kumar, A., (2017) *Mater Sci Eng C Mater Biol Appl.* 73:333-339
13. Zhang, D., Zhou, W., Wei, B., Wang, X., Tang, R., Nie, J., Wang, J., (2015) *Carbohydr Polym.* 125: 189-99.
14. Tian, H., Yan, J., Rajulu, A.V., Xiang, A., Luo, X., (2017) *Int J Biol Macromol.* 96:518-523.
15. Ruth, S.M., Poblete, S., Joy, L., Diaz, L., (2014) *Advanced Materials Research,* 925:379-384.
16. Tang, L., Huang, B., Wang, Q.U.S., Oua, W., Lina, W., Chena, X., (2013) *Bioresource Technology Volume* 127:100-105
17. Lin, S. Y., Chen, K. S., Run-Chu, L., (2001) *Biomaterials* 22: 2999.
18. Dussán, K. J., Silva, D. D. V., Moraes, E. J. C., Arruda, P. V., Felipe, M. G. A., (2014) 38:433-438.
19. Saito, T., Nishiyama, Y., Putaux, J. L., Vignon, M., Isogai, A., (2006) *Biomacromolecules*, 7 (6):1687-1691.
20. Cuia, S., Zhanga, B. S., Gea, S., Xionga, L., Suna, Q., (2016) 83:346-352.
21. Poletto, M., Ornaghi, H. L. Jr., Zattera, A. J., (2014) 7:6105-6119.
22. Kondo, T., (1997) *The assignment of IR absorption bands due to free hydroxyl groups in cellulose.* 4:281-292.
23. Ciolacu, D., Ciolacu, F., Popa, Y. I., (2011) 45(1-2): 13-21.
24. Kumar, A., Negi, Y.S., Bhardwaj, N. K., Choudhary, V., (2013) *Adv. Mat. Lett.* 4(8):626-631.
25. Johar, N., Ahmada, I., Dufresne, A., (2012) *Indus. Crop. Prod.* 37:93-99.
26. Tang, C.M., Tian, Y. H., Hsu, S. H., (2015) 8: 4895-4911.
27. Peppas, N. A., Korsmeyer, R. W., Boca Raton CRC Press (1986) 27-56.
28. Drużyńska, M. G., Czubenko, J. O., (2012) 17:59-66.
29. Bajpai, S. K., Daheriya, P., Ahuja, S., Gupta, K., (2016) *Designed Monomers and Polymers* 19(7).
30. Schott, H., (1992) *J. Macromol. Sci. Part B.* 31:1-9.